Grenze International Journal of Engineering and Technology, Jul Issue

3D Content-Based Retrieval for T1 Weighted Contrast Enhanced Magnetic Resonance Brain Database using Multiple Features

Dhanya K. Sudhish[1] and Latha R. Nair[2]
[1]Research Scholar, Division of Computer Science, School of Engineering, CUSAT, India.
[2]Associate Professor in CSE, Division of Computer Science, School of Engineering, CUSAT, India

***Abstract*—Advancement in medical imaging modality and the fast development of the internet is generating a larger database of high-resolution 3D Volumes of medical data. In the medical field, the Computer-aided systems that support disease diagnosis and correlation of different subjects with similar cases are of great application. Retrieval of 3D medical data with high resolution from a very large database, made the feature extraction of voxels, a vivid area of research. The paper exploits the efficiency of 3D wavelet transform and 3D Run-length matrices for representing volumetric texture feature. The system proposed an efficient 3D MRI scan retrieval from a 3D database, similar to the provided query. As for the retrieval precision, the proposed 3D CBR system achieves a precision rate of 90.12%. This paper evaluates the proposed CBIR system's performance, for the Euclidean and the Manhattan distance metric.**

***Index Terms*—3D, Content-Based Retrieval, 3D medical Data, 3D feature descriptors, 3D Discrete Wavelet Transform and 3D Run-Length Matrix.**

I. INTRODUCTION

The advancement in image acquisition techniques of the 3D models from real-world scenarios, and the 3D shapes generated by computer-aided modelling and visualizing, increased the volume of 3D domain-specific data. In many fields like engineering, medical diagnosis, and the educational sector, 3D models are of great application. In the recent years, the technical advancements of medical imaging equipment generated huge amounts of medical data. This large database of high-resolution medical images can be efficiently used for clinical diagnosis, decision making for treatment planners, and treatment progress evaluation.

The image quality of MRI data is improving in contrast and resolution, as the scanning technologies and scan parameters are evolving. Clinical practitioners depend mainly on Magnetic Resonance imaging, due to its excellence in spatial resolution and tissue contrast, especially for the brain images. Furthermore, MRI imaging works in the radio frequency range, and hence eliminates the risk of ionizing radiation involved in the other imaging modalities like CT (Computer-Aided Tomography) scan and Positron Emission Tomography (PET) scan.

In earlier days, to salvage the required images from databases, all the images were first annotated by text and then, a database retrieval method based on this text was used for the retrieval of the images. The text annotation of image content and metadata played a significant part in text-based retrieval methods in which the annotation was subjective and language-dependent[1]. The image retrieval based on word content was used initially in the

Grenze ID: 01.GIJET.7.2.505

works of Kato, in which a visual interaction mechanism was implemented on a conventional relational database system[2]. In a retrieval framework that is content-based, a query image is fed and relevant images are retrieved from the database. These frameworks help the users have an easier retrievability of the images from a large database, which is based on all visual contents that are present in the query image. In the paper[3], J. Kaur et al. presented a detailed review of various content-based systems, their extraction methods of visual contents from colour, texture, shape etc, and the formation of the feature database, using the feature vector extracted. In these systems, the low-level features like colour, texture and shapes are extracted automatically, and the feature vector from the query image is also extracted. Then the relational space between the images in the database and query image are computed, and the images with high feature similarity are retrieved as the visual output.

CBIR systems conceived in the medical domain are modality dependent task specific. CBIR can be useful to retrieve clinically relevant volumes from the large medical data archives, for disease progression analysis and also to compare similar observations among different patients. A CBIR framework includes preprocessing of image data, feature extraction, indexing, model learning, similarity checking, feedback-based retrieval and visualization.

This work proposes a CBIR system to retrieve clinically relevant cases for the diagnosis and treatment of the given image. A large database of MRI Brain scans is fed to the Feature Extraction(FE) module. The FE employed to get volumetric features are 3D WT (Wavelet transform) and 3D RLM (Run-length Matrix). The feature vector for each subject is extracted and then, the texture feature database is generated. When a query 3D volume comes, the feature-vector is extracted and compared with the records in the texture feature database. The retrieval module retrieves the 3D MRI volumes from the database for visualization. The distance metrics used for similarity measure are the Euclidean and the Manhattan distance.

II. Literature Review

In the paper [4], FE is done by Margin Information Descriptor, which can describe the features of neighbouring tissues of a tumor, for image content representation. The authors designed the Maximum Mean Average precision projection as a distance measuring metric. Classification of abnormal and normal brain MRI images in the database was done in [5] by extracting the texture details using Gobar filter and the classification was done by the Support Vector Machine (SVM). The work [6] proposes a brain parallelization tool to extract image features and use them for searching and evaluation. Here, the similarity is measured using image subtraction. A. Chaddad [7] modelled an automatic FE based on the Gaussian Mixture Model (GMM), for brain MRI. The accuracy performance for T1 weighted MRI and T2 weighted images were 97.05%, and FLAIR images accuracy reduced to 94.11%. In the paper, early detection of the Alzheimer's disease using a Computer-Aided system based on eigenbrain, and a sequential minimal optimization (SMO) is utilized, to train the support vector machine. A signature of feature for MRI image is done using a logistical regression model, to predict the Epidermal Growth Factor Receptors expression level in gliomas [8]. This signature consists of 15 textural features, one shape-based and one size-based feature, and 25 first-order statistics features. In the paper [9], the authors developed an image retrieval system that is content-based, and the bag-of-visual-words model is used to extract features. A distance learning algorithm, REML (Rank Error-based Metric Learning) is used to get a precision of 93.1%.

Traditional FE techniques for CBIR use handcrafted features for forming the feature vector. Z. Swati, et al. [10] proposed an FE framework based on VGG19, and the measurement of the distance similarity between an image query and the images in the database, using the CFLM (Closed-Form Learning method). The work done on CE-MRI dataset adopted the method of transfer/convey learning, and the retrieval performance was enhanced using a block-wise fine turning strategy. The spatial information forfeiture due to pooling and striding was reduced by using 3D atrous- convolution in the work [11] and a 3D fully connected conditional random field was developed for the post-processing. The research work in [12] defines a volumetric feature that is generated from the gradient information pulled out on the XYZ orthogonal plane at each voxel, based on the local coordinates system. The final feature is defined with the local 3D gradient generated by the proposed 3D gradient calculator and the local coordinate system. Hasan and Meziane[13] developed a bespoke grey level co-occurrence matrix, generated 9 matrices and computed 21 descriptors from each matrix, where each MRI brain data gave 183 descriptors that formed the texture feature vector, and finally achieved 97.8% accuracy. In the work [14], a 3D texture classification strategy is proposed using a sub-band filtering method, and a specialized feature selection strategy is developed, which reduces the dimension of the feature vector for classification, based on feature relevance. Research work [15] proposed a volumetric run-length encoder to capture the texture features from 3D medical data. A method to generate 3D texture analysis of MRI brain was proposed in [16] based on multiple sort co-occurrence matrix, exploiting the image features such as intensity, gradient and anisotropy.

III. System Architecture

The 3D Content-Based Image retrieval framework proposed here has an FE module, feature database, query processing module and retrieval and visualization module. Figure 1 shows the architecture of the presented 3D CBIR framework for the 3D MRI database.

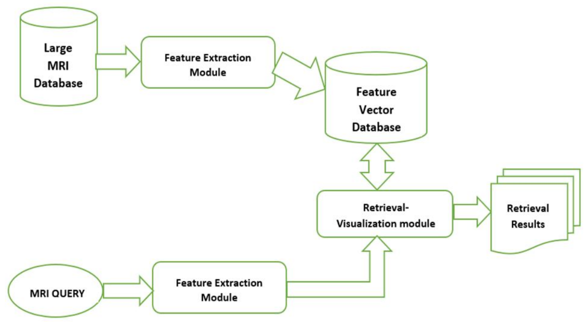

Fig: 1 3D CBIR Frame work

IV. Volumetric Feature Extraction

For the 3D Medical images, the inside texture features give the tissue properties of the volume of interest. The information content present in the texture features plays a significant role, in representing each 3D MRI brain subject in the database. In the earlier approaches, the extraction of 2D based texture features was done from the 3D dataset, as these data were stacks of 2D slices. Such 3D texture feature-based approaches suffer from the loss of interlaced information between the voxels.

A. 3D DWT features

The 3D wavelet transforms give the spatial and frequency information of voxels. For a 2D MRI Slice, the wavelet decomposition involves a recursive filtering with a low pass(L) and a high pass(H) filter in vertical and horizontal directions, followed by sub-sampling of each output images, generating LLn, LHn, HLn, and HHn . A 3D wavelet transform is done by applying low pass (L) and high pass (H) filters, along with the three dimensions generating 8 wavelet sub-bands. In the lower frequency sub-bands, the process is repeated to generate two-scale 3D wavelet coefficients[17].

The 3D WT feature is derived from the statistical measure; the mean (μ) and standard deviation (σ) of the wavelet coefficients in each sub-band for two-scales are computed. The 3D WT texture feature consists of 30 features ie. 2(scales) *7 (sub-bands in each scale) *2 (measures) +2(measures in the lowest resolution) =30 [17].

B. 3D RLM features

3D Run-length statics represent the unevenness of the texture of voxels in a specific direction. A run gives the string of consecutive pixels with the same grayscale intensity value along a linear direction. In the run-length matrix P, each P (i, j) gives the number of runs with pixels having grayscale intensity; i and j give the length of run in the d(x, y, z) direction. The displacement vector d(x, y, z) defines the orientation, where x, y and z represents the displacements along the x-axis, y-axis and z-axis respectively. From the possible 26 displacements in the three-dimensional space, the volumetric texture feature requires 13 displacements vectors in the directions (00, 450), (00,900), (00,1350), (450,450), (450,900), (450,1350), (900,450), (900,900), (900,1350), (1350,450), (1350,900), (1350,1350) and (-,00) with vector representation d(x, y ,z) as (1, 0, 1), (1, 0, 0), (1, 0, -1), (1, 1, 1), (1, 1, 0), (1, 1, -1), (0, 1, 1), (0, 1, 0), (0, 1, -1), (-1, 1, 1), (-1, 1, 0), (-1, 1, -1) and (0, 0, 1) respectively.

Eleven texture feature descriptors extract information from run-length matrices are short-run emphasis (SRE), high gray-level run emphasis (HGRE), long-run emphasis (LRE), low gray-level run emphasis (LGRE), the pair-wise combinations of the length and gray level emphasis (SRHGE, SRLGE, LRHGE, LRLGE,), run percentage (RPC), run-length non-uniformity (RLNU), and gray-level non-uniformity (GLNU) [15]. The FE employed to get volumetric features are 3D WT (Wavelet transform) and 3D RLM (Run-length Matrix). The feature vector for each subject is extracted and a feature vector database is built. When a 3D query volume comes, the feature vector is extracted and fed to the retrieval module, which ranks the 3D subjects in ascending order of similarity distances.

V. Implementational Details

The Dataset used to demonstrate the performance of this work is BRATS 2018[18]. It includes 210 HGG (High-Grade Glioma) subjects and 75 LGG (Low- Grade Glioma) subjects. The experiment is performed for 90 HGG subjects and 35 LGG subjects. The preprocessing steps by the BRATS Organizers include Co-registration, resampling and skull stripping. Each subject consists of four sequences of MRI scans, T1- weighted, T2-weighted, T1- Contrast and FLAIR. The dimension of each MRI data is 155x240x240 (Slice number x length x width), and all are stored as a signed 16-bit integer. The data fed to the proposed 3D CBIR is BRATS 2018 challenge, which includes 90 HGG cases and 35 LGG cases. The T1-Contrast MRI data of each patient is used for the experiment. Each MRI data is processed for volumetric FE and a feature vector is generated consisting of texture features, using the Feature extraction module. The Feature extraction module employs 3D WT and 3D RLM methods as feature generator methods. Each feature vector contains 41 features (30 features extracted using 3D WT and 11 descriptors using 3D RLM).

The FE module computes the feature vector database for the entire 3D MRI subjects. When the query volume comes, it is fed to the FE module to compute the feature vector for the query. The retrieval module takes the query feature vector, computes the distance of similarity between the data in the feature vector database and the query feature vector. The system retrieves similar 3D MRI data for visualization. The distance matrices used to compare the similarity among the data in the feature vector database and the query feature vector, are the Euclidean and the Manhattan distance metrics and the system performance for these two different similarity measures is evaluated.

$$\text{Euclidean distance} = \sqrt{\sum_{i=1}^{n}(x_i - y_i\,)^2} \qquad (1)$$

$$\text{Manhattan distance} = \sum_{i=1}^{n}|x_i - y_i| \qquad (2)$$

Where n is the dimension of the feature vector, X represents the query image and Y represents the images within the database.

VI. Performance Evaluation

The performance analysis of an image retrieval system that is content-based, is wisely measured using precision, recall and precision at k (*P@k*, k is the number of retrieved data) of the system. Precision, P is evaluated as the ratio of the number of retrieved relevant 3D models, to the total number of models retrieved. The recall is calculated as the ratio of the number of relevant images retrieved, to the total number of relevant images in the image database.

$$Precicion(P) = \frac{t_{positive}}{N_{retrieved}} = \frac{t_{positive}}{t_{positive}+f_{positive}} \qquad (3)$$

where *tpositive* is the number of relevant volumes retrieved, *fpositive* is the miss classified irrelevant images and *Nretrieved* is the total number of volumes retrieved.

$$Recall(R) = \frac{t_{positive}}{N_{relavant}} = \frac{t_{positive}}{t_{positive}+f_{negative}} \qquad (4)$$

where is the total number of relevant volumes in the database, and *fnegative* is relevant volumes but misclassified as irrelevant volumes. The precision takes into account all the retrieved images. The *p@k* gives the number of most relevant images in the top k retrieved images. The performance of our CBIR system is evaluated by precision, recall, P@10, P@15 and P@20. Table 1and Table 2 shows the retrieval performance of three FE methods, using the Euclidean and Manhattan distance metric. Table 1 shows the retrieval performance of the CBIR system with FE methods using 3D DWT, 3D RLM and the combined 3D DWT and 3D RLM, at *precision@k* (k=10,15,20). It is seen from Table 4 that the precision achieved by the feature fusion of 3D DWT and 3D RLM, outperforms the performance of FE using 3D DWT and 3D RLM separately.

TABLE I. RETRIEVAL PERFORMANCE CALCULATED AT P@10, P@15 AND P@20 OF 3D DWT, 3D RLM AND 3D DWT +3D RLM WHILE USING EUCLIDEAN SIMILARITY METRIC

	K=10	K=15	K=20
3D DWT	90.12	89.23	87.86
3D RLM	88.32	86.81	85.94
3D DWT +3D RLM	92.10	91.25	89.87

TABLE II. RETRIEVAL PERFORMANCE CALCULATED AT P@10, P@15 AND P@20 OF 3D DWT, 3D RLM AND 3D DWT +3D RLM WHILE USING MANHATTAN SIMILARITY METRIC

	K=10	K=15	K=20
3D DWT	89.56	88.47	87.01
3D RLM	86.21	85.11	83.98
3D DWT + 3D RLM	90.89	88.79	86.13

TABLE III. AVERAGE PRECISION OF 3D DWT, 3D RLM AND 3D DWT +3D RLM FOR HIGH-GRADE GLIOMA AND LOW-GRADE GLIOMA USING EUCLIDEAN DISTANCE

Tumor Grade	3D DWT	3D RLM	3D DWT + 3D RLM
HGG	90.72	89.63	93.53
LGG	89.52	87.01	90.67

TABLE IV. AVERAGE PRECISION OF 3D DWT, 3D RLM AND 3D DWT +3D RLM USING EUCLIDEAN DISTANCE

	3D DWT	3D RLM	3D DWT + 3D RLM
Average Precision (%)	90.12	88.32	92.10

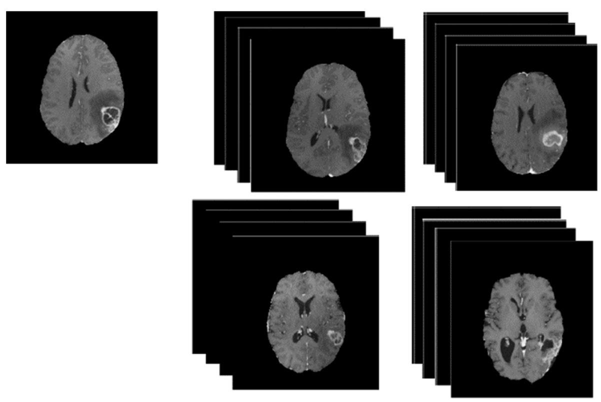

Fig 2. The retrieval result of an MRI query

VII. CONCLUSION

This paper proposed a 3D Content-Base Retrieval framework for retrieving 3D Magnetic Resonance scans of the brain, from a large MRI Brain Database. The retrieval scheme is classified into three, (i) the FE module to represent the 3D MRI database into a feature vector database, (ii) a query processing module which receives a query 3D MRI scan from the user and generates the feature vector and (iii) a retrieval and visualization module, which retrieve and visualize 3D MRI scans similar to the received query. The experiments are done on T1 weighted contrast enhanced MRI scans in the BRATS 2018 challenge. The FE module uses the robustness of both 3D WT and 3D RLM, for feature vector generation. The proposed system promises a precision rate of 90.12%, which is better when collated with the existing texture feature descriptors for CBIR methods.

REFERENCES

[1] M. Alkhawlani and M. Elmogy, “Text-based, Content-based, and Semantic-based Image Retrievals: A Survey,” International Journal of Computer and Information Technology, vol. 04, no. 01, pp. 58–66, 2015.

[2] T. Kato, “Database architecture for content-based image retrieval ages with each user .,” SPIE/IS &T 1992 Symposium on Electronic Imaging: Science and Technology, vol. 1662, no. March, pp. 112–123, 1992.
[3] J. Kaur and M. Kumar, “REVIEW PAPER ON CONTENT BASED IMAGE RETRIEVAL FOR DIGITAL IMAGES,” INTERNATIONAL JOURNAL OF RESEARCH IN COMPUTER APPLICATIONS AND ROBOTICS www.ijrcar.com, vol. 3, no. 9, p. 108112, 2015.
[4] W. Yang et al., “Content-based retrieval of brain tumor in contrast-enhanced MRI images using tumor margin information and learned distance metric,” Medical Physics, vol. 39, no. 11, pp. 6929–6942, 2012, doi: 10.1118/1.4754305.
[5] G. Gilanie, U. I. Bajwa, M. M. Waraich, Z. Habib, H. Ullah, and M. Nasir, “Classification of normal and abnormal brain MRI slices using Gabor texture and support vector machines,” Signal, Image and Video Processing, vol. 12, no. 3, pp. 479–487, 2018, doi: 10.1007/s11760-017-1182-8.
[6] A. v. Faria, K. Oishi, S. Yoshida, A. Hillis, M. I. Miller, and S. Mori, “Content-based image retrieval for brain MRI: An image-searching engine and population-based analysis to utilize past clinical data for future diagnosis,” NeuroImage: Clinical, vol. 7, pp. 367–376, 2015, doi: 10.1016/j.nicl.2015.01.008.
[7] A. Chaddad, “Automated Feature Extraction in Brain Tumor by Magnetic Resonance Imaging Using Gaussian Mixture Models,” Hindawi, vol. 2015, 2015.
[8] Y. Li et al., “MRI features can predict EGFR expression in lower grade gliomas: A voxel-based radiomic analysis,” European Radiology, vol. 28, no. 1, pp. 356–362, 2018, doi: 10.1007/s00330-017-4964-z.
[9] M. Huang et al., “Content-based image retrieval using spatial layout information in brain tumor T1-weighted contrast-enhanced MR images,” PLoS ONE, vol. 9, no. 7, pp. 1–13, 2014, doi: 10.1371/journal.pone.0102754.
[10] Z. N. K. Swati et al., “Content-Based Brain Tumor Retrieval for MR Images Using Transfer Learning,” IEEE Access, vol. 7, no. c, pp. 17809–17822, 2019, doi: 10.1109/ACCESS.2019.2892455.
[11] Z. Zhou, Z. He, and Y. Jia, “AFPNet: A 3D fully convolutional neural network with atrous-convolution feature pyramid for brain tumor segmentation via MRI images,” Neurocomputing, 2020, doi: 10.1016/j.neucom.2020.03.097.
[12] R. Maani, S. Kalra, and Y. H. Yang, “Robust volumetric texture classification of magnetic resonance images of the brain using local frequency descriptor,” IEEE Transactions on Image Processing, vol. 23, no. 10, pp. 4625–4636, 2014, doi: 10.1109/TIP.2014.2351620.
[13] A. M. Hasan and F. Meziane, “Automated screening of MRI brain scanning using grey level statistics,” Computers and Electrical Engineering, vol. 53, pp. 276–291, 2016, doi: 10.1016/j.compeleceng.2016.03.008.
[14] C. C. Reyes-Aldasoro and A. Bhalerao, “Volumetric texture description and discriminant feature selection for MRI,” Lecture Notes in Computer Science (including subseries Lecture Notes in Artificial Intelligence and Lecture Notes in Bioinformatics), vol. 2732, no. August, pp. 282–293, 2003, doi: 10.1007/978-3-540-45210-2_52.
[15] D. H. Xu, A. S. Kurani, J. D. Furst, and D. S. Raicu, “Run-length encoding for volumetric texture,” Proceedings of the Fourth IASTED International Conference on Visualization, Imaging, and Image Processing, pp. 534–539, 2004.
[16] V. A. Kovalev, F. Kruggel, H. J. Gertz, and D. Y. von Cramon, “Three-dimensional texture analysis of MRI brain datasets,” IEEE Transactions on Medical Imaging, vol. 20, no. 5, pp. 424–433, 2001, doi: 10.1109/42.925295.
[17] Gao, XGao, X., Qian, Y., Hui, R., Loomes, M., Comley, R., Barn, B., … Rix, J. (2010). Texture-Based 3D Image Retrieval for Medical Applications. Proceedings of IADIS International Conference E-Health et al., “Texture-Based 3D Image Retrieval for Medical Applications,” Proceedings of IADIS International Conference e-Health, pp. 101–108, 2010.
[18] B. H. Menze et al., “The Multimodal Brain Tumor Image Segmentation Benchmark (BRATS),” IEEE Transactions on Medical Imaging, vol. 34, no. 10, pp. 1993–2024, 2015, doi: 10.1109/TMI.2014.2377694.